



Synthesis and catalytic properties of TS-1 with mesoporous/microporous hierarchical structures obtained in the presence of amphiphilic organosilanes

Yohan Cheneviere, Frédéric Chieux, Valérie Caps, Alain Tuel *

IRCELYON, Institut de recherches sur la Catalyse et l'Environnement de Lyon, UMR 5256, CNRS-Université de Lyon 1, 2 Avenue Albert Einstein, 69626 Villeurbanne Cedex, France

ARTICLE INFO

Article history:

Received 23 September 2009

Revised 2 November 2009

Accepted 2 November 2009

Available online 16 December 2009

Keywords:

Mesoporous materials

Zeolite

TS-1

Oxidation

Catalytic activity

ABSTRACT

Titanosilicates TS-1 with mesoporous/microporous hierarchical structures have been synthesized in the presence of an organosilane surfactant. Highly porous crystals, with regular pores of ca. 2.5–3.5 nm diameter, are obtained under hydrothermal conditions similar to those used for the preparation of conventional catalysts. The organosilane has a great influence on the textural properties of TS-1, but does not significantly affect the amount and coordination of Ti species in the framework. Mesoporous TS-1 have been used as catalysts in various oxidation reactions with an aqueous H₂O₂ and their activity has been compared with those of a conventional TS-1 and a mesoporous amorphous TiMCM-41. Data show that mesoporous TS-1 does not possess the expected properties for hierarchical catalysts, i.e. the properties of the conventional catalysts with advantages of mesoporous solids. In particular, the gain in diffusion due to intracrystalline mesopores is totally inhibited by the increase of the hydrophilic character of the zeolite, resulting from very high silanol group populations on the external surface.

© 2009 Elsevier Inc. All rights reserved.

1. Introduction

TS-1, the titanium-substituted silicalite-1, is one of the most efficient catalysts for the oxidation of small organic molecules with dilute hydrogen peroxide [1–9]. The unique activity of TS-1 has been attributed to (i) isolated, tetrahedrally coordinated Ti species in the framework, (ii) the hydrophobic character of the surface, and to a lesser extent (iii) the topology of the MFI framework that favors specific architectures for active Ti centers [10]. However, the pore opening of TS-1 limits the applications to small molecules, typically linear alkanes or alkenes, or monosubstituted aromatic compounds such as phenol, anisole, and aniline. For this reason, diffusion limitations are of particular importance, and it was reported that a slight increase in the crystal size could drastically affect the activity [11,12]. Molecular transport in zeolite channels can be improved by decreasing the particle size or by creating additional meso/macro porosity. The creation of intracrystalline porosity is an elegant strategy, since the corresponding zeolites combine the major advantages of micro and mesoporous materials. Primary approaches involved conventional dealumination by acid leaching or steaming at high temperature [13–16]. More recently, selective desilication of zeolites in basic media proved to be

efficient, but both the amount and size of mesopores were difficult to control [17–20].

Better results were obtained by generating intracrystalline mesoporosity during the synthesis of the zeolite. The crystallization can be performed in the presence of a removable nanostructured template such as carbon particles or polymer beads [21–30]. This process provides a rather good control of pore size and distribution but average pore sizes are quite large (≥ 10 nm), with broad distributions. Alternatively, zeolites with intracrystalline tunable porosity have been prepared with organosilanes, acting as both silica source and porogen agent. The obtained zeolites possess relatively small mesopores (2–10 nm) with narrow pore size distributions [31,32].

In contrast to aluminum-containing ZSM-5, studies on mesoporous TS-1 are rather scarce. The first example was reported by Jacobsen's group who prepared TS-1 in the presence of carbon black [33]. They showed that mesoporous TS-1 possessed approximately the same catalytic activity as conventional TS-1 in the oxidation of 1-octene but strongly surpassed the latter for the epoxidation of cyclohexene. It was argued that the superior activity of TS-1 could be attributed to improved diffusional properties and a better accessibility to the active sites. Later, mesoporous TS-1 has been prepared in the presence of various porogen agents, including hard templates (nanoporous carbons), or ethanolamine [34,35]. In all these papers, the benefit of an additional porosity is generally deduced from a comparison of catalytic performances in reactions involving large molecules, for which conventional TS-1 is not active. More interesting would be to compare mesoporous zeolites

* Corresponding author. Present address: KAUST Catalysis Center (KCC), 4700 King Abdullah University of Science and Technology, Thuwal 23955-6900, Saudi Arabia. Fax: +33 472 445 399.

E-mail address: alain.tuel@ircelyon.univ-lyon1.fr (A. Tuel).

with catalysts active in these reactions, for example Ti-containing mesoporous silicas. Moreover, the influence of the mesoporosity on the intrinsic properties of TS-1 in classical reactions, such as phenol hydroxylation, has never been clearly reported.

The present paper reports the synthesis, characterization, and catalytic performance of mesoporous TS-1 prepared in the presence of amphiphilic organosilanes. These zeolites have been compared with the conventional TS-1 and TiMCM-41 in a series of reactions involving both small and large substrates. The aim of the work was not only to correlate the activity with the presence of mesopores, but also to try to answer some of the fundamental questions:

- Does the additional porosity modify the activity in reactions for which conventional TS-1 is an excellent catalyst?
- Is mesoporous TS-1 more or less active than TiMCM-41 in reactions involving large molecules?
- Is there any influence of the “crystallinity” of the pore walls on the activity?

2. Experimental

2.1. Synthesis of the catalysts

Mesoporous TS-1 samples (further denoted MesoTS-1) were prepared using the commercial organosilane [3-(trimethoxysilyl)propyl]octadecyldimethylammonium chloride, TPOAC, 72 wt.% solution) from Aldrich. The synthesis was adapted from that used by Choi and coworkers for the preparation of mesoporous AlZSM-5 [31]. In a typical preparation, 30 mL H₂O was mixed with 37 mL alkali-free TPAOH (1 M solution, prepared by ion exchange of TPABr with Ag₂O). Then, 22.5 mL tetraethyl orthosilicate (TEOS, Aldrich) was added and the mixture was stirred for 1 h. Then, 0.52 mL tetrapropyl orthotitanate (TPOT) in 5 mL isopropanol was added dropwise. After the addition of titanium, 3.65 mL TPOAC was added and the resulting mixture, with the following composition 1 SiO₂–0.05 TPOAC–0.015 TiO₂–0.37 TPAOH–33 H₂O, was heated at 80 °C for 3 h under stirring to remove alcohol formed upon the hydrolysis of the alkoxides. The gel was then transferred in a stainless-steel, Teflon-coated autoclave and was crystallized under rotation (60 rpm) at 145 °C for different periods. After crystallization, solids were recovered by centrifugation, washed with distilled water and air-dried at 100 °C for 12 h. Organic molecules (both TPA and the long-chain surfactant) were then removed from the pores by calcination in air at 550 °C.

A conventional TS-1 was prepared using the same gel composition (Si/Ti = 67) in the absence of TPOAC.

TiMCM-41 was prepared from very dilute gels, following the method reported by Lin et al [36]. Typically, 1.24 g NaOH was dissolved in 2.115 l H₂O, followed by the addition of 4.155 g CTABr. Then, a solution containing 22.5 mL TEOS and 0.52 mL TPOT was added dropwise under very vigorous stirring and stirring was maintained for 2 h more at room temperature. Then, the solid was recovered by filtration, washed with water, and dried at 100 °C for 12 h. TiMCM-41 was then calcined in air flow at 550 °C for 16 h. The solid possessed all the characteristics of a hexagonal mesoporous silica (typical reflections in the XRD pattern) with a mean pore size of 3.2 nm, as evidenced from N₂ adsorption/desorption isotherm.

2.2. Characterization

All catalysts have been characterized by X-ray diffraction on a Bruker (Siemens) D 5005 diffractometer, using Cu K α_2 radiation.

Information on the meso-structure of TiMCM-41 and MesoTS-1 was obtained from diffractograms recorded between 0.5° and 10° (2 θ), with steps of 0.02° and 5 s per step. Standard diffractograms (2 θ from 3° to 80°, 1 s per step) were used to evaluate the crystallinity of zeolitic catalysts MesoTS-1 and TS-1.

UV–Vis spectra were recorded on a Perkin Elmer Lambda 35 spectrometer equipped with an integration sphere.

N₂ adsorption/desorption isotherms were collected at liquid nitrogen temperature using a Micromeritics ASAP 2010 apparatus. Before the measurement, approximately 50 mg of the sample was dehydrated under vacuum (10^{–3} Torr) at 350 °C overnight.

TEM pictures were taken on a Jeol 2010 Microscope with an accelerating voltage of 200 kV.

NMR spectra were obtained on a Bruker DSX 400 spectrometer equipped with a double-bearing probe-head. The samples were spun at 10 kHz in 4 mm zirconia rotors. ¹³C NMR spectra were recorded using a conventional ¹H–¹³C cross-polarization sequence with 2 ms contact time and 10 s recycle delay. Chemical shifts were referenced to tetramethylsilane (TMS).

Ti contents were obtained by ICP-AES after dissolution of the corresponding zeolites in HF:HCl solutions.

2.3. Catalytic reactions

2.3.1. Oxidation of 2,6-di-tert-butylphenol (DTBP)

The oxidation of DTBP was carried out batch-wise in a round-bottomed flask equipped with a condenser and a magnetic stirrer. In a typical reaction, 200 mg of catalyst was dispersed in a solution containing 19 mL of acetone and 2.06 g (0.01 mol.) of DTBP. When temperature was stabilized at 70 °C, 3 mL of a 35 wt.% H₂O₂/H₂O solution (29 × 10^{–3} mol H₂O₂) was added in one lot. The samples were then periodically taken and analyzed by GC using a 30 m × 0.32 mm × 0.25 μ m Varian column filled with CP-WAX 52 CB.

2.3.2. Hydroxylation of phenol

The hydroxylation of phenol was carried out using the same equipment as that used for the oxidation of DTBP. Typically, 10 g of phenol was dissolved in 10 mL of methanol containing 200 mg of catalyst. The mixture was vigorously stirred (900 rpm) and the temperature was increased to 70 °C. Then, an amount of hydrogen peroxide (35 wt.% solution) corresponding to a ratio H₂O₂/phenol = 0.2 was added in one lot.

2.3.3. Epoxidation of cyclohexene

Cyclohexene (1 mmol) was dissolved in 20 mL of methylcyclohexane and the mixture was heated at 70 °C under stirring. Then 56 mg of catalysts was added, followed by 5 × 10^{–3} mol anhydrous TBHP (96 wt.% in decane). The samples were periodically taken and analyzed by a Shimadzu GC-2014 using an Equity TMS column (30 m × 0.25 mm × 0.25 μ m). The equipment was similar to that used for the other reactions.

3. Results

3.1. Influence of synthesis parameters on structural and chemical properties

For an organosilane with a given chain length, crystallization time and temperature have a great influence on the structural properties of the final zeolite. It has been reported that both the mean diameter and distribution of mesopores increased with time and that narrow pore size distributions could only be obtained at short crystallization periods or low temperature [31]. The evolution of the porosity, which results from a crystal ripening process,

can be controlled by lowering temperature. In the particular case of AlZSM-5, the mesopore diameter could be stabilized at 3.1 nm even after 12 days if the synthesis was performed at 130 °C instead of 150 °C. TS-1 is generally synthesized at quite high temperatures, typically 170–180 °C [37]. Preliminary experiments performed at 175 °C did not allow us to obtain narrow pore size distributions along with crystalline zeolites. The liquid phase recovered after crystallization was brown, suggesting a partial degradation of organosilane molecules during the hydrothermal process. The temperature was thus decreased to 145 °C, which was sufficiently high to obtain highly crystalline TS-1 within relatively short periods. Under such conditions, the organosilane, which concentration was fixed to 5% with respect to TEOS, remained intact during crystallization, as evidenced by solid-state NMR analysis of the final solid.

The influence of crystallization time on the structural properties of TS-1 has been studied by collecting solids after different periods, from 4 h to 6 days. The evolution of XRD patterns (at both low and high angle values) supports the gradual transformation of an amorphous mesoporous Ti-silicate into a crystalline zeolite (Fig. 1). After four hours, reflections characteristic of the MFI framework are not yet detected but a broad line is observed around 2°. Zeolite peaks appear after 15 h and their intensity continuously grows until approximately 4 days. At the same time, the reflection at 2–3° decreases and shifts to high angle values, indicating a gradual transformation of the mesoporous structure. Clearly, the presence of the organosilane, even at low concentration, strongly affects the crystallization kinetics: the same experiment performed in the absence of TPOAC led to a highly crystalline TS-1 within 20 h. The crystallization of the zeolite significantly modifies the composition of the solid. The Ti content increases from ca. 0.87% in the amorphous solid recovered after 4 h to 1.2% in the zeolite crystallized for 6 days (Table 1). This corresponds to a variation of the Si/Ti ratio in dried calcined solids from 85 to 60, these values being quite close to the theoretical Si/Ti ratio (Si/Ti = 67).

Amorphous catalysts recovered during the initial crystallization period ($t < 15$ h) show sponge-like networks without any regular size and shape (Fig. 2). The morphology drastically changes with zeolite crystallization. After 3 days, highly porous regular particles, with the typical habit of twinned ZSM-5 crystals, are formed. Amorphous domains that were prevailing at short synthesis times ($t < 15$ h) have completely disappeared, suggesting that these domains are progressively dissolved under alkaline conditions and provide the necessary species for zeolite crystal growth.

The evolution of solids with time has also been monitored by ^{13}C solid-state NMR. After 4 h, the solid does not contain zeolite crystals and the NMR spectrum corresponds to TPOAC molecules only (Fig. 3). Additional peaks around 10, 17, and 63 ppm appear on the spectra of solids recovered after longer crystallization periods and they can be assigned to TPA molecules. Moreover, the splitting of the peak at 10 ppm indicates that TPA groups are occluded in the MFI framework. This fingerprint of MFI-type zeolites results from different environments of propyl chains in the straight and sinusoidal channels of the structure [38,39]. Although NMR intensities are not directly proportional to the number of carbon atoms in ^1H - ^{13}C CP/MAS experiments, it was possible to estimate the relative proportions of TPOAC and TPA molecules in the series of solids by comparing NMR intensities in the 20–40 and 0–20 ppm ranges. NMR signals between 20 and 40 ppm correspond to 16 –(CH_2)– groups of the aliphatic chain of TPOAC molecules, whereas signals at 10 and 17 ppm result from 4 –(CH_2 – CH_3) moieties of TPA⁺ cations. For a better estimation, the minor contribution of TPOAC molecules between 0 and 20 ppm was systematically subtracted from all spectra. Fig. 4 shows that the amount of TPOAC is approximately constant up to 1 day and that it rapidly decreases as the zeolite crystallizes. Simultaneously, the amount of TPA

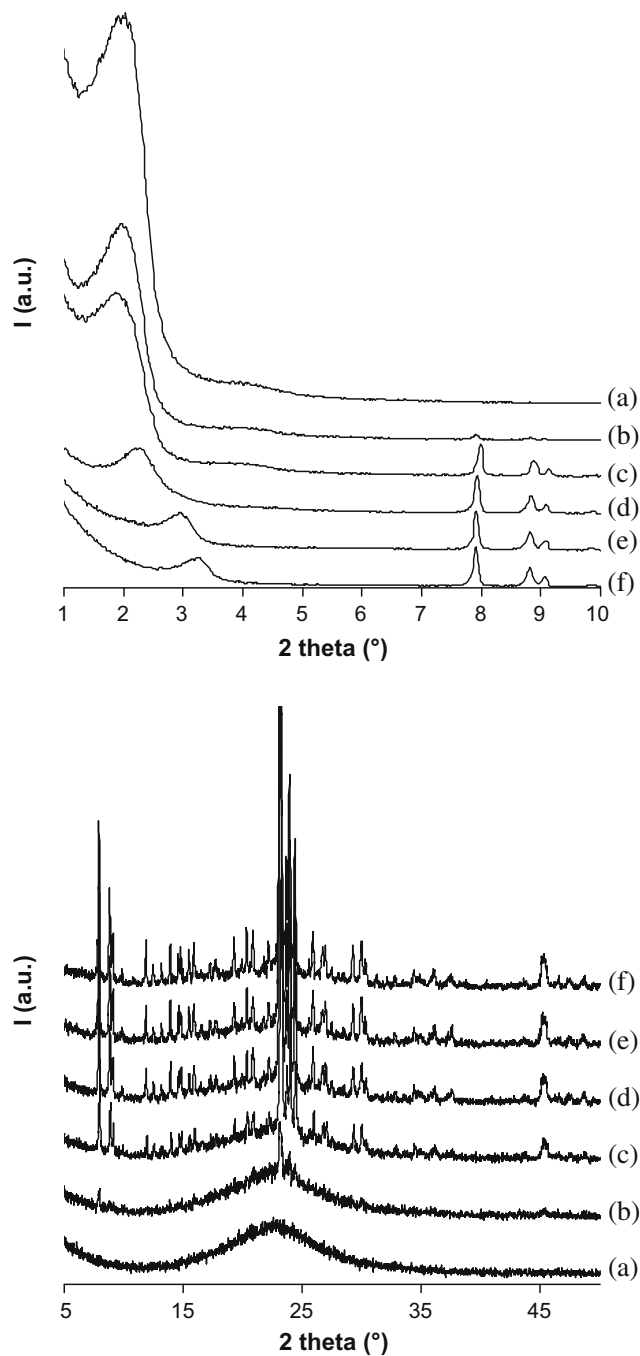


Fig. 1. Low angle (top) and high angle (bottom) X-ray diffraction patterns of samples recovered after various crystallization times: 4 h (a), 15 h (b), 1 day (c), 2 days (d), 4 days (e), and 6 days (f).

increases, and fits perfectly the crystallinity of the zeolite deduced from XRD. After 4 days we could estimate a TPA/TPOAC molar ratio close to 2. The decrease of TPOAC concentration after one day supports the dissolution of the primary amorphous mesoporous solid, thus providing silica species for zeolite crystallization.

The evolution of the BET surface area of the solids is also consistent with the transformation of an amorphous material into a crystalline zeolite. Indeed, it decreases from ca. 1050 m^2/g after 4 h to 550 m^2/g after 4 days (Table 1). For comparison, a standard TS-1 obtained at 145 °C for 48 h has a BET surface area of 437 m^2/g , clearly showing the existence of an additional porosity in the samples prepared with TPOAC. Short crystallization periods led to

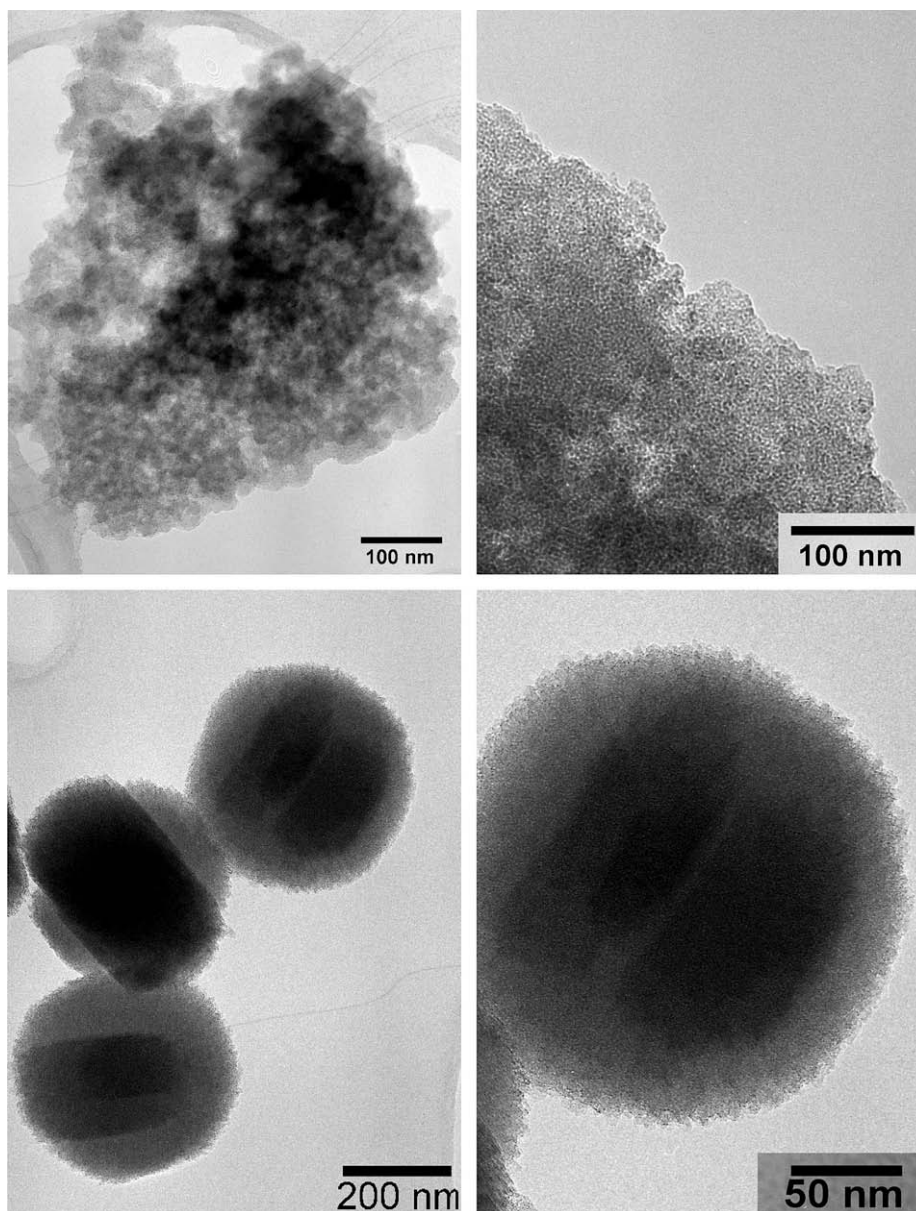


Fig. 2. TEM pictures of solids recovered after 4 h (top) and 3 days (bottom).

type-IV N_2 isotherms with an abrupt step at p/p_0 around 0.3, characteristic of mesoporous solids with regular pore openings. Moreover, t -plot curves indicate that solids recovered after 4 and 15 h are almost exclusively mesoporous, in agreement with the absence of zeolitic material (Table 1). Increasing the crystallization period

gradually shifts the step to higher pressure values, decreases the mesopore volume and broadens the pore size distribution (Table 1). The mean pore size varies from 2.4 nm after 4 h to 3.5 nm after 6 days. The variation is somewhat limited as compared to that reported for ZSM-5 catalysts prepared at 150 °C [31].

Table 1
Chemical composition and structural characteristics of the samples.

Sample	Crystallization time	Ti (wt.%)	S_{BET} (m^2/g)	V_{meso} (cm^3/g) ^a	Φ_p (nm) ^b	Crystallinity (%) ^c
TS-1 Meso	4 h	0.87	1034	1.05	2.4	0
TS-1 Meso	15 h	0.97	885	0.87	2.7	23
TS-1 Meso	1 day	1.09	774	0.62	3.0	64
TS-1 Meso	2 days	1.22	683	0.28	3.2	87
TS-1 Meso	4 days	1.21	545	0.21	3.4	93
TS-1 Meso	6 days	1.21	544	0.19	3.4	100
TS-1	2 days	1.22	437	0.08	–	–

^a Total volume of pores with diameter >2 nm.

^b Pore diameter obtained by BJH method on the desorption branch of the isotherm.

^c Crystallinity measured on the high angle part of XRD patterns.

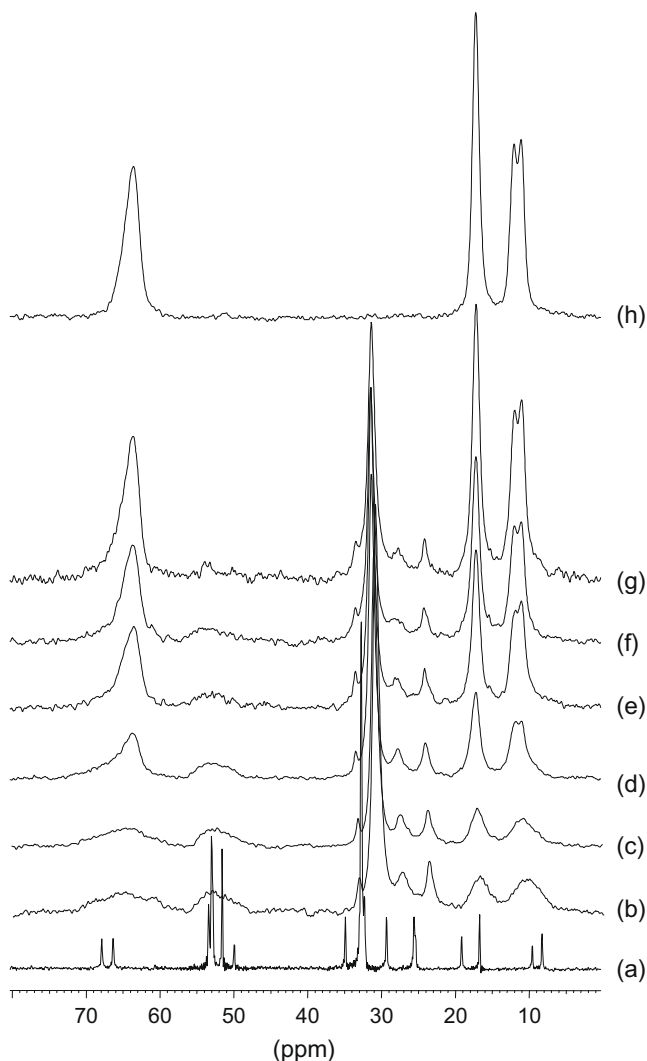


Fig. 3. Solid-state ^1H - ^{13}C CP/MAS NMR spectra of the as-synthesized solids recovered after 4 h (b), 15 h (c), 1 day (d), 2 days (e), 4 days (f), and 6 days (g). For comparison, NMR spectra of the amphiphilic surfactant (a) and of a pure TS-1 prepared in the absence of TPOAC (h) are also reported.

Solids recovered at different periods between 4 h and 6 days have been characterized by UV–Vis spectroscopy in the dehydrated state. The technique gives direct information about the nature and coordination of Ti species in silica networks [40,41]. Before crystallization of the zeolite, a broad band is observed between 200 and 350 nm, with a maximum centered at ca. 240 nm (Fig. 5). As far as the crystallization of the zeolite proceeds, the band width decreases, and the maximum shifts to higher energies. After one day, both the position of the maximum (approx. 225 nm) and the line width (line width at half maximum LWHM \approx 60 nm) remained practically unchanged. The broad peak observed after 4 h is a characteristic of Ti-containing mesoporous silicas such as TiMCM-41 and Ti-HMS [42,43]. It was attributed to a charge transfer between oxygen and Ti atoms, simultaneously present in tetra, penta, and hexacoordinated structures. As previously reported, similar bands have also been observed for very small nanometric oxide clusters on silica [44]. However, the absence of signal above 300 nm suggests that large extraframework TiO_2 particles with a structure similar to anatase are not present. The evolution of UV–Vis spectra with time strongly supports the zeolite crystallization, with a gradual change in Ti coordination. However, the signals of solids recovered after 1 day differ from that of a conventional TS-1, prepared in

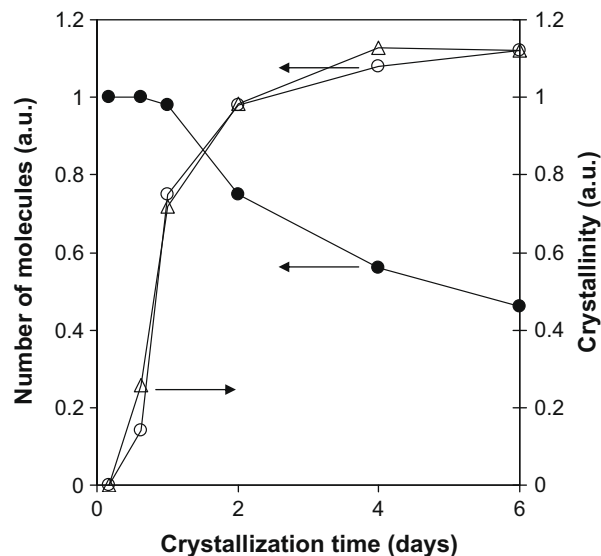


Fig. 4. Evolution with crystallization time of the relative number of amphiphilic surfactant molecules (\bullet) and TPA molecules (\circ) in as-made solids, deduced from NMR spectra. For comparison, the crystallinity of the solids, calculated from XRD intensities, is also reported (Δ).

the absence of TPOAC. Indeed, pure TS-1 shows a maximum at 210 nm, with a LWHM smaller than 40 nm. This band is characteristic of a $\text{O}(2p) \rightarrow \text{Ti}(3d)$ charge transfer transition, and is generally taken as a “fingerprint” for the isolated, tetrahedrally coordinated $\text{Ti}(\text{OSi})_4$ species in hydrophobic zeolite frameworks. For mesoporous TS-1 materials, the maximum at ca. 220 nm suggests the simultaneous presence of tetrahedral tripodal $\text{Ti}(\text{OSi})_3\text{OH}$ and tetrapodal $\text{Ti}(\text{OSi})_4$ Ti species [10]. The slight difference between conventional and mesoporous zeolites clearly indicates that the presence of TPOAC during crystallization influences the dispersion and/or coordination of Ti species.

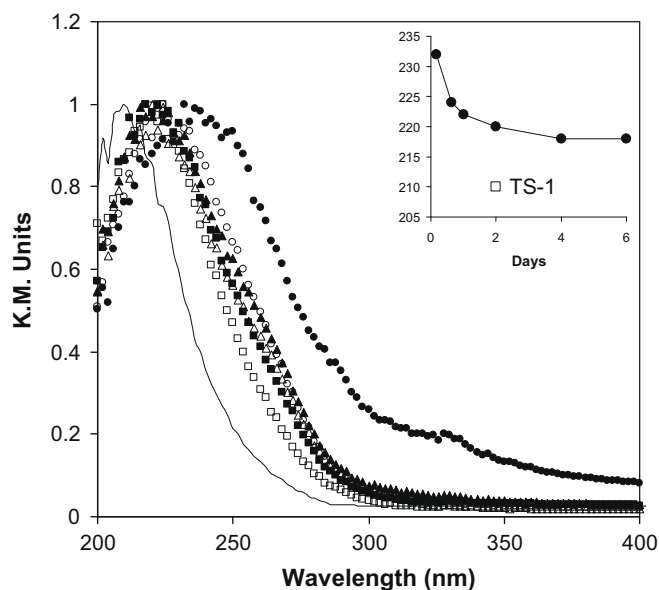


Fig. 5. UV–Vis spectra of MesoTS-1 recovered at various crystallization times: 4 h (\bullet), 15 h (\circ), 1 day (\blacktriangle), 2 days (\triangle), 4 days (\blacksquare), and 6 days (\square). For comparison, the spectrum of a conventional TS-1 prepared in the absence of TPOAC is also reported (full line). Inset: position of the maximum of UV–Vis spectra with time, and comparison with a conventional TS-1 (\square).

3.2. Catalytic activity

3.2.1. Oxidation of 2,6-di-*tert*-butylphenol (DTBP)

DTBP is a large molecule that cannot penetrate the micropores of the MFI structure and, consequently, cannot be oxidized over TS-1. By contrast, good to excellent results have been reported using mesoporous catalysts containing Ti or Zr and dilute hydrogen peroxide as an oxidant [45,46]. In this case, it seems that the presence of the isolated, tetrahedrally coordinated species is not a necessary condition to activate H_2O_2 and oxidize the molecule and that the hydrophilic character of amorphous silica has no detrimental effect on the reaction.

As expected, TiMCM-41 is active in the reaction: approximately 60% of DTBP is converted after 3 h, with selectivity in di-*tert*-butylbenzoquinone (DTBQ) close to 85%. The other product is 3,3',5,5'-tetra-*tert*-butyldiphenylquinone (DPQ), a bimolecular compound formed from 2,6-di-*tert*-butylphenoxy radicals. When using the microporous TS-1 as a catalyst, only 2% of DTBP is converted, which confirms that the catalytic sites are inside micropores and are not accessible to the molecule. Due to its amorphous and mesoporous nature, the solid recovered after 4 h is highly active (Fig. 6). Both the conversion (63%) and selectivity are quite similar to those obtained over TiMCM-41. This is also the case for the solid obtained after 15 h, though the conversion is somewhat lower and reaches only 38%. However, the activity drastically falls down when TS-1 crystallizes, and solids recovered after two days or more are not more active than a standard TS-1.

3.2.2. Hydroxylation of phenol

The hydroxylation of phenol to dihydroxybenzenes is one of the reactions that largely contributed to the interest of the scientific community to reactions catalyzed by TS-1. It does not only produce catechol (*ortho*-dihydroxybenzene) and hydroquinone (*para*-dihydroxybenzene) in excellent yields, but it is also very sensitive to reaction parameters and catalyst structure. In particular, a combination between isolated Ti(IV) sites and hydrophobic zeolite channels seems to be a necessary condition for high conversions and DHB selectivities. Moreover, the phenol conversion depends on the crystal size, and the creation of an additional porosity is expected to have a strong influence on the activity [47]. A “blank” experiment was performed using a conventional catalyst, prepared in the absence of TPOAC. After 6 h, 19% of the initial amount of phenol was converted into ca. 6% catechol, 11.5% hydroquinone,

and 1.5% tars. The *para*:*ortho* ratio is close to 1.9, which is the expected value for reactions performed in methanol [12].

Phenol conversions obtained after 6 h on the series of mesoporous TS-1 catalysts are reported in Table 2. For catalysts crystallized for 4 and 15 h, the very low conversion is not surprising since these catalysts are similar to TiMCM-41, which is known to be inactive in this reaction, mainly because of the hydrophilic character of the surface. The low activity for the catalysts recovered after longer periods is more unexpected, particularly when they appear to be zeolitic solids by XRD. Actually, the reaction mixture becomes dark a few minutes after the addition of hydrogen peroxide and only traces (max. 1.5%) of the *ortho* isomer are detected.

3.2.3. Epoxidation of cyclohexene

The real benefit of an intracrystalline mesoporosity on the activity in cyclohexene epoxidation with H_2O_2 was first observed on mesoporous TS-1 crystallized in the presence of carbon beads. After one hour, the mesoporous catalyst produced approx. 10 times more cyclohexene oxide than a conventional TS-1, which was attributed to a better accessibility of the active sites [33].

One of the mesoporous zeolites prepared with TPOAC has been used as a catalyst in the epoxidation of cyclohexene with an anhydrous *tert*-butyl hydroperoxide (TBHP) and compared not only with a conventional TS-1, but also with an amorphous mesoporous TiMCM-41. As expected, the activity of the conventional TS-1 is low and the yield in cyclohexene oxide reaches only 3.5% after 6 h (Fig. 7 and Table 3). By contrast, TiMCM-41 is active in this reaction, yielding 30% cyclohexene oxide after 6 h. For the mesoporous TS-1 crystallized in the presence of TPOAC for 3 days, both the activity and epoxide yield are similar to those obtained over TiMCM-41, which indicates that the amorphous/crystalline nature of the catalyst walls (and, in turn, the Ti centers geometry) has minor influence in this reaction. The use of aqueous hydrogen peroxide as an oxidant in this reaction considerably decreased the activity and the epoxide yield, clearly showing the negative influence of water in the reaction (Table 3).

4. Discussion

From characterization techniques, catalysts prepared with TPOAC show a strong analogy with the conventional TS-1. In

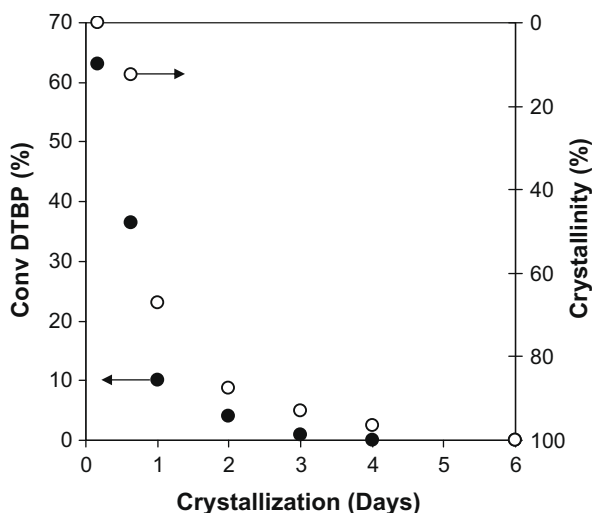


Fig. 6. Conversion in the oxidation of di-*tert*-butyl phenol with H_2O_2 and crystallinity of the catalysts as a function of synthesis time.

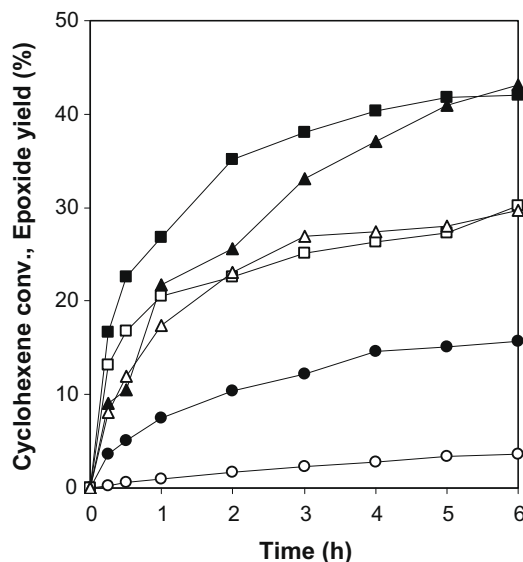


Fig. 7. Cyclohexene conversion (black symbols) and cyclohexene oxide yield (open symbols) over MesoTS-1 recovered after 3 days (■, □), TiMCM-41 (▲, △), and conventional TS-1 (●, ○).

Table 2
Hydroxylation of phenol over various catalysts.

Sample	Crystallization time	Conv. PhOH (%)	Conv. H ₂ O ₂ (%)	HQ (%)	CAT (%)
TS-1 Meso	4 h	0.9	34	–	0.6
TS-1 Meso	15 h	1.0	30	–	0.6
TS-1 Meso	1 day	1.3	45	0.2	0.7
TS-1 Meso	2 days	1.2	38	–	0.7
TS-1 Meso	4 days	1.6	48	0.3	0.6
TS-1 Meso	6 days	1.5	32	0.3	0.8
TS-1	2 days	18	100	5.7	11.5

Reaction conditions: 10 g phenol, 10 ml methanol, 200 mg catalyst, H₂O₂:phenol = 0.2, T = 70 °C.

Table 3
Epoxidation of cyclohexene over various catalysts.

Catalyst	Oxidant	Cyclohexene conv. (%)	Yield (%)		
			Epoxide	Ketone	Alcohol
TS-1	TBHP	16.6	3.6	0	0.4
TiMCM-41	TBHP	43	29.8	0	0.75
TS1-Meso	TBHP	43	30.1	0	0.7
TS1-Meso	H ₂ O ₂	19	1.6	0	1.8

Reaction conditions: 1 mmol cyclohexene, 20 ml methylcyclohexane, 56 mg catalyst, 5×10^{-3} mol anhydrous TBHP.

particular, the presence of the isolated, tetrahedrally coordinated Ti species in the MFI framework type suggests similar environments for titanium sites and, consequently, similar properties. Catalytic data clearly show that this is not true, and that mesoporous TS-1 does not combine the properties of the conventional TS-1 with advantages of mesoporous solids. Mesoporous TS-1 can be regarded as a network of zeolite nanoparticles (<5 nm) with a quite regular inter-particle porosity (Fig. 2). At short synthesis times, Ti sites are quite easily accessible to large molecules, as they are in amorphous silicas such as TiMCM-41, which is clearly demonstrated by the high activity of the corresponding solids in the oxidation of DTBP with H₂O₂. The formation of zeolitic nanocrystals requires the partial dissolution of the mesoporous amorphous phase and recrystallization in the presence of TPA⁺ cations. Crystallization of MFI zeolites from MCM-41 type materials has already been reported previously. This route leads to conventional, non-porous zeolite crystals, from which surfactant molecules are completely excluded [48]. In the case of syntheses performed with TPOAC, surfactant molecules are linked to inorganic species, with a chemical bond stable in basic aqueous solutions. As a consequence, zeolite growth is disrupted by the presence of non-hydrolysable Si–C bonds and the particle size is limited to a few nanometers. However, as far as the zeolite forms, both Si and Ti species are involved in the crystallization process and catalytic sites are confined in micropores. The transition of Ti atoms from amorphous mesopores to crystalline micropores is perfectly illustrated by changes in UV–Vis spectra. The blue-shift of the maximum along with the decrease of the line width with time is consistent with a decrease in Ti coordination, induced by crystalline zeolite micropores. After zeolite crystallization, Ti sites become no longer accessible to bulky molecules and we observe a dramatic decrease of the activity in the oxidation of DTBP. Moreover, the very low conversion suggests that the surface of TS-1 nanocrystals do not possess a huge amount of catalytic sites, or that these sites are inactive.

More surprising is the lack of activity of the solids in the hydroxylation of phenol. It has been widely reported that this reaction is limited by diffusion of reactants and/or products in zeolite micropores and that the activity increases with decreasing the crystal size [11]. However, the crystal size is not the only factor that can affect the activity of Ti-containing zeolites. Indeed, at-

tempts to oxidize phenol with H₂O₂ over Ti-Beta zeolites have never been very successful even on Al-free catalysts, despite a Ti environment very similar to that existing in TS-1 [49,50]. The difference with TS-1 has been attributed to the hydrophilic character of Beta zeolite, resulting from a high concentration of defect sites in the framework. It has been postulated that zeolites crystals form from more or less disordered structures and that the crystallinity increases with growth [51,52]. Consequently, zeolite nanocrystals possess a high “defect probability” compared to large crystals, which is generally revealed by quite broad reflections in XRD patterns. Mesoporous TS-1 zeolites contain a huge amount of silanol groups, as evidenced by an intense band around 3740 cm⁻¹ in the infra red spectrum (not shown). The band is approx. 3 times more intense than that observed on a conventional TS-1 and similar to that observed on TiMCM-41. In the presence of an aqueous hydrogen peroxide, both the surface and internal sites of the zeolite are covered with water, which prevents the accessibility to phenol molecules and greatly reduces the reaction rate.

In order to check whether water is effectively responsible for the absence of reaction with aqueous H₂O₂, the epoxidation of cyclohexene has been performed over mesoporous TS-1 under quasi non-aqueous conditions, using an anhydrous TBHP as an oxidant. The high activity of the solid crystallized for 3 days shows that mesoporous TS-1 really contains active sites, capable of oxidizing cyclohexene in the presence of an anhydrous TBHP. However, these sites are very sensitive to water and they become totally inactive in the presence of hydrogen peroxide. The difference in activity with a conventional TS-1 can be attributed either to the very small size of TS-1 particles, making diffusion easier in liquid phase reactions, or to specific sites on the external surface of the catalyst, that do not exist on TS-1. Reactions involving bulky molecules over mesoporous AlZSM-5 have recently evidenced the role of surface sites in the activity [53,54]. Interestingly, these sites possess an acid strength different from that of Brønsted sites in the conventional ZSM-5 catalysts. Density functional theory (DFT) calculations showed that the acid strength of Brønsted acid sites located on the mesopore walls is modified by the presence of Al–OH and Si–OH defect sites. For mesoporous TS-1, the presence of numerous Si–OH groups may not only increase the hydrophilic character of the zeolite, but also modify the intrinsic properties of neighboring Ti centers on both the external and internal zeolite surface, making them inactive in structure-sensitive reactions such as phenol hydroxylation.

5. Conclusion

Highly porous TS-1 zeolites have been obtained by adding an amphiphilic organosilane to a conventional synthesis route. The organic molecule strongly influences the structural properties of the zeolite: it creates intracrystalline additional porosity, with pore diameters in the range of 2.5 – 3.5 nm. Mesopores are separated by crystalline walls, as evidenced by X-ray diffraction, the properties of which are very similar to those of the conventional TS-1

catalysts. In particular, the Ti content and coordination are not affected by the presence of the organosilane, Ti sites being essentially tetrahedrally coordinated in the zeolite framework. Additional intracrystalline mesoporosity is expected to improve the accessibility of active sites to bulky molecules such as substituted aromatics. This is effectively the case in the epoxidation of cyclohexene: the activity of mesoporous TS-1 is similar to that of an amorphous TiMCM-41 when the reaction is performed in the absence of water, which suggests that the input of potentially active sites on the external surface is negligible. However, when the substrate is too large to penetrate the zeolite micropores, the benefit of an additional porosity is negligible and mesoporous TS-1 behaves like a conventional catalyst. In the case of phenol hydroxylation, intracrystalline mesopores have a very negative impact on the activity. The creation of mesopores is accompanied by a considerable development of the external surface area, which generates many silanol groups and increases the hydrophilic character of the zeolite. In the presence of aqueous hydrogen peroxide solutions, the intrinsic activity of Ti sites is modified by water molecules, which is not the case in the hydrophobic micropores of the conventional TS-1 catalysts. The absence of activity in the hydroxylation of phenol with H₂O₂ clearly shows that mesoporous TS-1 does not possess the expected properties for hierarchical catalysts, i.e. the properties of conventional catalysts with advantages of mesoporous solids. Equilibrium between crystal size and surface composition has to be found to ensure that the gain in diffusion is not inhibited by a high hydrophilic surface, due to a huge population of silanol groups.

References

- [1] U. Romano, A. Esposito, F. Maspero, C. Neri, M.G. Clerici, *Stud. Surf. Sci. Catal.* 55 (1990) 33.
- [2] A.V. Ramaswamy, S. Sivasanker, *Catal. Lett.* 22 (1993) 239.
- [3] G. Perego, G. Bellussi, C. Corno, M. Taramasso, F. Buonomo, A. Esposito, *Stud. Surf. Sci. Catal.* 28 (1986) 129.
- [4] I.W.C.E. Arends, R.A. Sheldon, M. Wallau, U. Schuchardt, *Angew. Chem. Int. Ed. Engl.* 36 (1997) 1144.
- [5] B. Notari, *Stud. Surf. Sci. Catal.* 37 (1987) 413.
- [6] U. Romano, A. esposito, F. Maspero, C. Neri, M.G. Clerici, *La Chimica et L'Industria* 72 (1990) 610.
- [7] G.J. Hutchings, D.F. Lee, A.R. Minihan, *Catal. Lett.* 39 (1996) 83.
- [8] S. Gontier, A. Tuel, *Appl. Catal. A: Gen.* 118 (1994) 173.
- [9] M.G. Clerici, in: S. David Jackson, Justin S.J. Hargreaves (Eds.), *Metal Oxide Catalysis*, vol. 2, 2009, p. 705.
- [10] P. Ratnasamy, D. Srinivas, H. Knözinger, *Adv. Catal.* 48 (2004) 1. and references therein.
- [11] A.J.H.P. van der Pol, A.J. Verduyn, J.H.C. van Hooff, *Appl. Catal. A: Gen.* 92 (1992) 113.
- [12] A. Tuel, Y. Ben Täarit, *Appl. Catal. A: Gen.* 102 (1993) 69.
- [13] U. Lohse, H. Stach, H. Thamm, A.A. Schirmer, A.A. Isirikylan, N.I. Regen, M.M. Dubinin, *Z. Anorg. Chem.* 460 (1980) 179.
- [14] R. Dutartre, L.C. de Menorval, F. Di Renzo, D. McQueen, F. Fajula, P. Schulz, *Micropor. Mater.* 6 (1996) 311.
- [15] S. Donk, A.H. Jansen, J.H. Bitter, K.P. Jong, *Catal. Rev.* 45 (2003) 297.
- [16] M. Ogura, S.H. Shinomiya, J. Tateno, Y. Nara, E. Kikuchi, M. Matsukata, *Chem. Lett.* (2000) 882.
- [17] J.C. Groen, L.A.A. Peffer, J.A. Moulijn, J. Perez-Ramirez, *Colloids Surf. A* 241 (2004) 53.
- [18] J.C. Groen, J.C. Jansen, J.A. Moulijn, J. Perez-Ramirez, *J. Phys. Chem. B* 108 (2004) 13062.
- [19] J.C. Groen, L.A.A. Peffer, J.A. Moulijn, J. Perez-Ramirez, *Micropor. Mesopor. Mater.* 69 (2004) 29.
- [20] J.C. Groen, T. Bach, U. Ziese, A.M. Paulaime-van-Donk, K.P. de Jong, J.A. Moulijn, J. Perez-Ramirez, *J. Am. Chem. Soc.* 127 (2005) 10792.
- [21] J.C.H. Jacobsen, C. Madsen, J. Houzvicka, I. Schmidt, A. Carlsson, *J. Am. Chem. Soc.* 122 (2000) 7116.
- [22] Y.S. Tao, H. Kanoh, K. Kaneko, *J. Am. Chem. Soc.* 125 (2003) 6044.
- [23] K. Egeblad, M. Kustova, S.K. Klitgaard, K. Zhu, C.H. Christensen, *Micropor. Mesopor. Mater.* 101 (2007) 214.
- [24] X. Wei, P.G. Smirniotis, *Micropor. Mesopor. Mater.* 89 (2005) 170.
- [25] Y. Tao, H.K. Kanoh, K. Kaneko, *J. Phys. Chem. B* 107 (2003) 10974.
- [26] A. Sakthivel, S.-J. Huang, W.-H. Chen, Z.-H. Lan, K.-H. Chen, T.-W. Kim, R. Ryoo, A.S.T. Chiang, S.-B. Liu, *Chem. Mater.* 16 (2004) 3168.
- [27] H. Li, Y. Sakamoto, Z. Liu, T. Ohsuna, O. Terasaki, M. Thommes, S. Che, *Micropor. Mesopor. Mater.* 106 (2007) 174.
- [28] I. Schmidt, A. Boisen, E. Gustavsson, K. Stahl, S. Pehrson, S. Dahl, A. Carlsson, C.J.H. Jacobsen, *Chem. Mater.* 13 (2001) 4416.
- [29] B.T. Holland, L. Abrams, A. Stein, *J. Am. Chem. Soc.* 121 (1999) 4308.
- [30] X. Yang, Y. Feng, G. Tian, Y. Du, X. Ge, Y. Di, Y. Zhang, B. Sun, F.-S. Xiao, *Angew. Chem. Int. Ed.* 44 (2005) 2563.
- [31] M. Choi, H.S. Cho, R. Srivastava, C. Venkatesan, D.-H. Choi, R. Ryoo, *Nat. Mater.* 5 (2006) 718.
- [32] H. Wang, T. Pinnavaia, *Angew. Chem. Int. Ed.* 45 (2006) 7603.
- [33] I. Schmidt, A. Krogh, K. Wienberg, A. Carlsson, M. Brorson, C.J.H. Jacobsen, *Chem. Commun.* 21 (2000) 2157.
- [34] Y. Fang, H. Hu, *Catal. Commun.* 8 (5) (2007) 817.
- [35] X. Ke, L. Xu, C. Zeng, L. Zhang, N. Xu, *Micropor. Mesopor. Mater.* 106 (2007) 68.
- [36] K. Lin, P. Pescarmona, H. Vandepitte, D. Liang, G. van Tendeloo, P. Jacobs, *J. Catal.* 254 (2008) 64.
- [37] M. Taramasso, G. Perego, B. Notari, *U.S. Pat.* 4,410,501, 1983.
- [38] J. B'Nagy, Z. Gabelica, E.G. Derouane, *Zeolites* 3 (1983) 43.
- [39] S.L. Burkett, M.E. Davis, *Chem. Mater.* 7 (1995) 920.
- [40] A. Zecchina, S. Bordiga, C. Lamberti, G. Ricchiardi, D. Scarano, G. Petrini, G. Leofanti, M. Mantegazza, *Catal. Today* 32 (1996) 97.
- [41] M.R. Boccuti, K.M. Rao, A. Zecchina, G. Leofanti, G. Petrini, *Stud. Surf. Sci. Catal.* 48 (1989) 133.
- [42] S. Gontier, A. Tuel, *Zeolites* 15 (1995) 601.
- [43] K. Chaudhari, D. Srinivas, P. Ratnasamy, *J. Catal.* 203 (2001) 25.
- [44] A. Tuel, L.G. Hubert-Pfalzgraf, *J. Catal.* 217 (2003) 343.
- [45] P.T. Tanev, M. Chibwe, T. Pinnavaia, *Nature* 368 (1994) 321.
- [46] S. Gontier, A. Tuel, *Appl. Catal. A: Gen.* 143 (1996) 125.
- [47] Y. Wang, A. Tuel, *Micropor. Mesopor. Mater.* 102 (2007) 80.
- [48] L. Huang, W. Guo, P. deng, Z. Xue, Q. Li, *J. Phys. Chem. B* 104 (13) (2000) 2817.
- [49] L.H. Callanan, R.M. Burton, U. Wilkenhoener, E. van Steen, *Stud. Surf. Sci. Catal.* 154 (C) (2004) 2596.
- [50] U. Wilkenhoener, G. Langhendries, F. van Laar, G.V. Baron, D.W. Gammon, P.A. Jacobs, *J. Catal.* 203 (1) (2001) 201.
- [51] J.R. Agger, N. Hanif, M.W. Anderson, *Angew. Chem. Int. Ed.* 40 (2001) 4065.
- [52] M.W. Anderson, J.R. Agger, N. Hanif, O. Terasaki, *Micropor. Mesopor. Mater.* 48 (2001) 1.
- [53] K. Suzuki, Y. Aoyagi, N. Katada, M. Choi, R. Ryoo, M. Niwa, *Catal. Today* 132 (2008) 38.
- [54] V.S. Shetti, J. Kim, R. Srivastava, M. Choi, R. Ryoo, *J. Catal.* 254 (2008) 296.